

REPORT



Half-life extension and non-human primate pharmacokinetic safety studies of i-body AD-114 targeting human CXCR4

Katherine Griffiths^a, Uli Binder^b, William McDowell^c, Rita Tommasi^d, Mark Frigerio^e, William G. Darby^{a,e}, Chris G. Hosking^{a,e}, Lionel Renaud^f, Matthias Machacek^f, Peter Lloyd^g, Arne Skerra^{b,h}, and Michael Foley^{a,e}

^aThe Department of Biochemistry and Genetics, La Trobe Institute for Molecular Science, La Trobe University, Bundoora, Melbourne, Australia; ^bXL-protein GmbH, Freising, Germany; ^cAbzena, Babraham Research Campus, Cambridge, UK; ^dLonza Biologics, Slough, UK; ^eAdAlta Limited, Bundoora, Australia; ^fLYO-X GmbH, Basel, Switzerland; ^gKinDyn Consulting Limited, West Sussex, UK; ^hLehrstuhl für Biologische Chemie, Technische Universität München, Freising, Germany

ABSTRACT

Single domain antibodies that combine antigen specificity with high tissue penetration are an attractive alternative to conventional antibodies. However, rapid clearance from the bloodstream owing to their small size can be a limitation of therapeutic single domain antibodies. Here, we describe and evaluate the conjugation of a single domain i-body, AD-114, which targets CXCR4, to a panel of half-life extension technologies including a human serum albumin-binding peptide, linear and branched PEG, and PASylation (PA600). The conjugates were assessed in murine, rat and cynomolgus monkey pharmacokinetic studies and showed that the branched PEG was most effective at extending circulating half-life in mice; however, manufacturing limitations of PEGylated test material precluded scale-up and assessment in larger animals. PA600, by comparison, was amenable to scale-up and afforded considerable half-life improvements in mice, rats and cynomolgus monkeys. In mice, the circulating half-life of AD-114 was extended from 0.18 h to 7.77 h following conjugation to PA600, and in cynomolgus monkeys, the circulating half-life of AD-114-PA600 was 24.27 h. AD-114-PA600 was well tolerated in cynomolgus monkeys at dose rates up to 100 mg/kg with no mortalities or drug-related clinical signs.

ARTICLE HISTORY

Received 31 January 2019
Revised 23 May 2019
Accepted 27 May 2019

KEYWORDS

Half-life extension; i-body; PA600; PEGylation; CXCR4; pharmacokinetics

Introduction

Biological macromolecules are a major drug class that offer several advantages over traditional small molecule drugs. Combining high affinity and high selectivity typically results in reduced off-target and adverse effects of biological therapeutics. These features have facilitated the development of numerous therapeutic monoclonal antibodies (mAbs) that now stand-alone as an important class of commercially successful drugs.¹ However, mAbs are glycosylated, have a complex multi-domain structure and a high molecular weight, which can make their manufacture difficult and costly. Furthermore, they do not efficiently penetrate tissue, and since they tend to interact with their target antigen over a large flat footprint, are also limited in their ability to target functional regions of proteins such as active sites and ligand binding sites. Next-generation antibody fragments and antibody-like molecules can overcome some of these limitations. For example, they are generally smaller and simpler proteins, and some, such as the nanobody,² V_{NAR}³ and i-body,⁴ possess long binding loops that enable penetration into functionally important regions of proteins. This latter feature means that these molecules may have novel and unique pharmacology that can be exploited in a therapeutic setting.^{5,6} While these features of protein-based therapeutics are crucial to their success as drugs, systemic residence time is an important

characteristic that affects the therapeutic window of the biomolecule, and thus determines whether it will become a successful drug.

The circulating half-life ($t_{1/2}$) of therapeutic proteins sized <50 kDa, such as single domain antibodies, is typically minutes to hours.⁷ This rapid clearance from the bloodstream is attributable to renal filtration, protease degradation and sometimes overall charge of the therapeutic protein, and is undesirable from the perspective that frequent drug administration is required to sustain steady and effective circulating concentrations in the patient.⁸ Of the numerous recombinant therapeutic molecules clinically available, half-life extension has been accomplished by a range of modifications,⁸ including: 1) increasing the effective hydrodynamic volume by fusion to PEG,^{9,10} fusion to unstructured proteins such as Pro/Ala-rich sequences (PASylation[®])¹¹ or XTEN[™],¹² or by glycosylation;¹³ and 2) engineering capability for binding to the neonatal Fc receptor (FcRn), which enables recycling of the therapeutic back into the bloodstream, via fusion to Fc,¹⁴ IgG¹⁵ or albumin.¹⁶

The single domain i-body AD-114 binds specifically and with high affinity to the G-protein coupled C-X-C chemokine receptor 4, CXCR4.⁴ CXCR4 is a high-value therapeutic target implicated in various cancers, fibroses,^{17,18} invasion by human immunodeficiency virus,¹⁹ and stem cell mobilization.²⁰ We have recently demonstrated that CXCR4 is upregulated in

CONTACT Michael Foley  M.Foley@latrobe.edu.au

 Supplemental data for this article can be accessed on the [publisher's website](#)

© 2019 The Author(s). Published with license by Taylor & Francis Group, LLC.

This is an Open Access article distributed under the terms of the Creative Commons Attribution-NonCommercial-NoDerivatives License (<http://creativecommons.org/licenses/by-nc-nd/4.0/>), which permits non-commercial re-use, distribution, and reproduction in any medium, provided the original work is properly cited, and is not altered, transformed, or built upon in any way.

lung tissue from idiopathic pulmonary fibrosis (IPF) patients, and that AD-114 inhibits human IPF fibroblast cell migration and collagen 1 production and ameliorates fibrotic lung remodeling in a murine model of lung fibrosis.⁶ With a view to developing the therapeutic potential of AD-114, we describe here the systematic analysis of a panel of AD-114 variants following modification with a range of validated half-life extension technologies. We show that AD-114 is amenable to and retains target-binding activity following the various C-terminal modifications and describe pharmacokinetic (PK) and half-life data acquired in mice, rats and cynomolgus monkeys. We report that, of the modifications tested, conjugation to PEG and PA600 moieties most significantly increased the circulating half-life, but that overall production yields were greatest when AD-114 was expressed recombinantly as a fusion with PA600. In extensive non-human primate (NHP) PK and safety studies, we determined that AD-114-PA600 had a terminal half-life of 25 h and was well tolerated under a variety of dosing regimens, including intravenous (IV), subcutaneous (SC), intraperitoneal (IP) delivery, repeat daily and weekly dosing and dose escalation up to 100 mg/kg.

Results

Engineering of half-life-extended AD-114 variants

In a murine PK study, the unmodified i-body, AD-114-Im7-FH, had a very short half-life ($t_{1/2}$) of 0.18 h (11 min) (Table 1). We, therefore, applied two approaches to increase the circulation time of the molecule. In the first approach, we engineered

binding capability to the major blood protein, human serum albumin (HSA), via integration of the SA21 peptide. Whilst in the second approach, we conjugated the i-body with either PEG (30 K linear and 2×20 K branched) or the intrinsically unstructured PAS polypeptide PA600.¹¹ AD-114-PA600 was produced in *E. coli* with and without His₆ as a C-terminal purification tag. Schematics for the various formats are shown in Figure 1a.

SA21 is an 18-mer peptide with binding affinities for rat, rabbit and human serum albumin of 266, 320 and 467 nM, respectively.²¹ Surface plasmon resonance (SPR) revealed that AD-114-Im7-SA21 produced in *E. coli* had an affinity of ~518 nM for HSA, which is consistent with the result reported by Dennis *et al.*²¹ AD-114-Im7 lacking the SA21 peptide had no measurable affinity for HSA (data not shown). SPR analysis demonstrated that none of the C-terminal alternations appreciably decreased AD-114 affinity for CXCR4, as all variants showed a binding constant of ~1 nM for immobilized lipoparticles harboring human CXCR4 (Table 2). Of note, the addition of PEG appeared to increase the affinity principally by improving the on rate, as measured by SPR. AD-114 variants (except for AD-114-Im7-SA21) also bound CXCR4⁺ Jurkat T cells (Supplementary S1), as demonstrated by flow cytometric analysis (Figure 1b).

Pharmacokinetic analysis in mice, rats and cynomolgus monkeys

IV, IP or SC injection with all AD-114 variants was clinically well tolerated in mice, rats, and cynomolgus monkeys, and did

Table 1. Pharmacokinetic summary of i-body conjugates in mice, rats and cynomolgus monkeys. Animals were dosed with i-body conjugates via the intravenous (IV), intraperitoneal (IP) or subcutaneous (SC) administration route. $T_{1/2}$ and t_{max} values were obtained from *in vivo* pharmacokinetic studies by non-compartmental analysis of the mean plasma concentration.

I-body conjugate	Animal model	N (number of animals)	Dose rate (mg/kg)	Admin. route	$t_{1/2}$ (h) \pm S.D.	t_{max} (h) \pm S.D.	C_{max} (μ g/mL) \pm S.D.	AUC_{last} (μ g-hr/mL)
AD-114-Im7-FH	mouse	3 ^b	3	IV	0.18 ^a	0.08	16.28	4.7
AD-114-Im7-FH-SA21	mouse	3 ^b	2	IV	0.95	0.08	20.53	25
AD-114-Im7 PEG 30K	mouse	3 ^b	3	IV	11.85	0.08	76.65	496
AD-114-Im7 PEG 2x20K	mouse	3 ^b	1.25	IV	19.24	0.08	25.44	381
AD-114-PA600-6H	mouse	3 ^b	10	IV	7.77 ^a	0.03	467	1871
		3 ^b		IP	7.03	2.00	176	1435
		3 ^b		SC	10.25	8.00	32.17	760
AD-114-PA600	rat	3 ^b	3.5	IV	9.5	0.083	114.7	681
		3 ^b		SC	NC ^c	24.00	4.79	194
AD-114-PA600-6H	Cyn. monkey	3	2	IV	24.27 \pm 0.24	0.17 \pm 0.29	84.12 \pm 22.04	393 \pm 69
Single dose study		2		SC	25.41 \pm 5.17	6.00 \pm 2.83	5.33 \pm 1.53	210 \pm 22
AD-114-PA600	Cyn. monkey	3	3 (Day 1)	IV	10.2 \pm 3.9	0.08 \pm 0	117 \pm 8.8	421 \pm 344
Dose escalation study			10 (Day 8)		6.7 \pm 1.1	0.08 \pm 0	369 \pm 9.9	2072 \pm 537
			30 (Day 15)		12.9 \pm 4.5	0.08 \pm 0	956 \pm 155.5	13740 \pm 10773
AD-114-PA600	Cyn. monkey	1	0.1 (Day 1)	SC	23.53	8	1279	37635
Dose escalation study			1 (Day 8)		14.76	8	3630	133332
			100 (Day 15)		NC	120	48686	6273094
		1	0.3 (Day 1)	SC	21.42	8	518	29899
			3 (Day 8)		8.31	24	8119	304347
			10 (Day 15)		11.73	24	9040	634861
AD-114-PA600		3	10 (Day 1)	IV	NC	0.083 \pm 0	430.9 \pm 84.3	1957 \pm 623
Repeat dosing study			(Day 7)		11.5 \pm 3.8	0.083 \pm 0	346.3 \pm 27.3	1662 \pm 615
		3	10 (Day 1)	SC	NC	16.0 \pm 8.7	27.4 \pm 8.7	521 \pm 173
			(Day 7)		15.9 \pm 11.5	2.8 \pm 2.0	82.5 \pm 47	1578 \pm 745
		3	30 (Day 1)	SC	NC	13.3 \pm 10.1	113.8 \pm 35.8	2205 \pm 702
			(Day 7)		20.6 \pm 13.1	6.7 \pm 4.6	190.6 \pm 54.2	4008 \pm 1122

^aData previously published by Griffiths *et al.* (2018)⁶ shown here for comparison to related variants.

^bError on PK values could not be determined as each animal was not bled at every timepoint.

^cThe $t_{1/2}$ could not be calculated due to the absence of at least 3-time points in the terminal elimination phase.

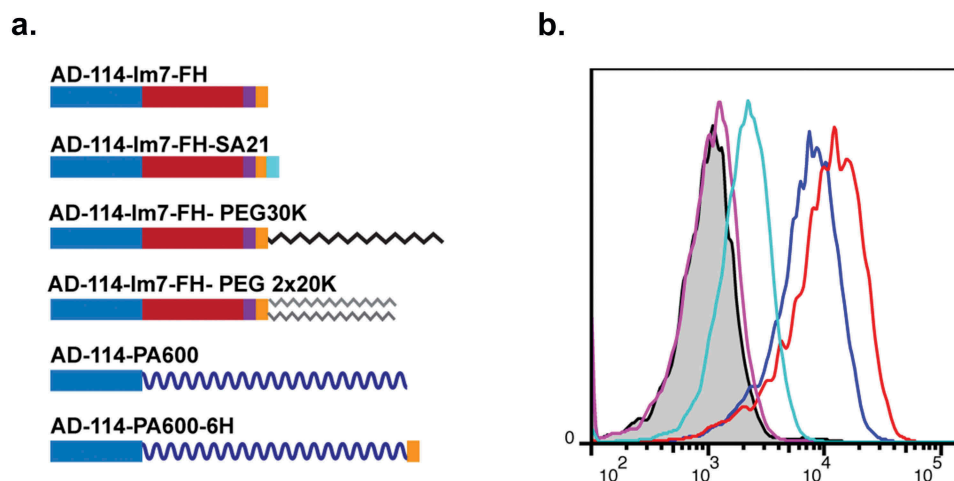


Figure 1. Attributes of AD-114 half-life-extended conjugates.

Various conjugates were added at the C-terminus of AD-114 (blue) to improve circulating half-life (Im7-FH, red; SA21 peptide, cyan; PEG 30K, black zig-zag; PEG 2 × 20K, grey zig-zags; PA600, blue ribbon). Purification tags were His₆ hexapeptide (orange) and FLAG peptide (purple) (a). Jurkat cells expressing CXCR4 were treated with AD-114 conjugates and visualized by flow cytometry: negative i-body (shaded), AD-114-Im7-FH-SA21 (pink), AD-114-Im7-FH-PEG 30K (cyan), AD-114-Im7-FH (blue), AD-114-PA600-6H (red) (b).

Table 2. The molecular weight of i-body variants was determined by mass spectrometry or by *in silico* prediction, binding kinetics were determined by SPR.

I-body conjugate	Molecular weight (Da)	Binding kinetics determined by SPR					
		Human CXCR4			Human serum albumin		
		Affinity K_D (nM)	Assoc. rate constant $k_a \times 10^5$ ($M^{-1}s^{-1}$)	Dissoc. rate constant $k_d \times 10^{-3}$ (s^{-1})	Affinity K_D (nM)	Assoc. rate constant $k_a \times 10^5$ ($M^{-1}s^{-1}$)	Dissoc. rate constant $k_d \times 10^{-3}$ (s^{-1})
AD-114-Im7-FH	24747 ^a	9.1	3.0	2.7	BLD ^e	BLD	BLD
AD-114-Im7-FH-SA21	26856 ^c	9.2	2.1	2.0	518	0.47	24.6
AD-114-Im7-FH-PEG 30K	54747 ^f	0.7	21.0	1.39	NA ^d		
AD-114-Im7-FH-PEG 2 × 20K	64747 ^f	0.7	22.0	1.48			
AD-114-PA600	59642 ^a	4.0	7.4	2.9			
AD-114-PA600-6H	60661 ^a	5.2 ^b	9.9	5.1			

^aDetermined by mass spectrometry.

^bPreviously reported.⁶

^cPredicted *in silico*.

^dNot assessed.

^eBelow level of detection.

^fPredicted weight based on mass of AD-114-Im7-FH + 1 × PEG moiety.

not result in any mortalities, test item-related clinical signs or significant changes in body weight.

When AD-114-Im7-FH-SA21 and the two PEGylated formats were assessed in a murine PK study with dosing via the IV route, all three modified formats had a longer $t_{1/2}$ than the unmodified AD-114-Im7-FH. The addition of SA21 correlated only with a small improvement in $t_{1/2}$ to 0.95 h (57 min), whereas PEG-30K and PEG 2 × 20K significantly extended the $t_{1/2}$ to 11.85 and 19.24 h, respectively (Figure 2, Table 1).

We have previously reported a $t_{1/2}$ of 7.77 h for mice dosed IV with 10 mg/kg of AD-114-PA600-6H.⁶ Due to a manufacturing advantage of AD-114-PA600 over the other half-life-extended formats, further PK and safety studies were subsequently undertaken with this i-body format in mice, rats, and non-human primates.

Analysis of AD-114-PA600 was initially extended to dosing mice at 10 mg/kg via the IP and SC routes, revealing $t_{1/2}$ values of 7.03 and 10.25 h, respectively. The t_{max} for IP and SC routes was 2 and 8 h, respectively (Figure 3, Table 1).

PK analyses were next conducted in rats and cynomolgus monkeys (*Macaca fascicularis*). In rats dosed IV with AD-114-

PA600 at 3.5 mg/kg, we observed a $t_{1/2}$ of 9.5 h (Figure 3, Table 1). When dosed SC at 3.5 mg/kg, a $t_{1/2}$ value could not be calculated due to the absence of >3 time points in the terminal elimination phase, but a t_{max} was observed at 24 h (Figure 3, Table 1).

Four NHP studies were then conducted. In the first study, animals were dosed with AD-114-PA600-6H via the IV and SC routes at 2 mg/kg. When administered IV, circulating levels of AD-114-PA600-6H decreased steadily over time, resulting in a $t_{1/2}$ of 24.27 h (Table 1). When administered SC, the slower absorption resulted in a lower C_{max} , as expected, and a longer t_{max} (6 h) compared with the IV dose, with a terminal $t_{1/2}$ of 25.41 h (Table 1) and detectable i-body in serum up to 192 h post-dose (~10 ng/mL for IV dosing and ~50 ng/mL for SC dosing) (Figure 4). Analysis of collective pooled IV data from the NHP studies showed that AD-114-PA600 conformed well to a linear, two-compartmental PK model.

In the second and third NHP studies AD-114-PA600 was administered in a dose escalation manner with IV dosing at 3, 10, then 30 mg/kg (Table 1, Figure 5a), or with SC dosing at

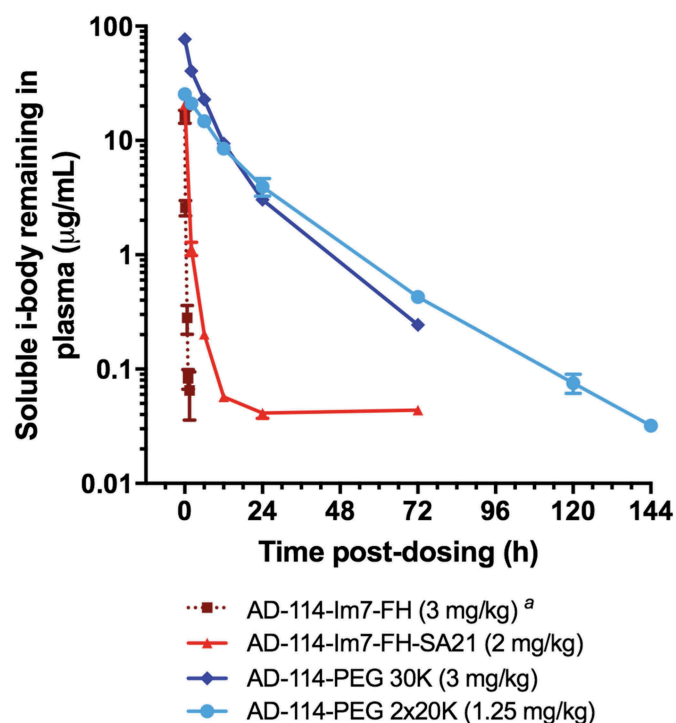


Figure 2. *In vivo* pharmacokinetic data from mice dosed with various half-life extended i-body conjugates via the intravenous (IV) route; showing decrease in the plasma concentration of i-body over time. $N = 3$, error bars show S.E.^a Data previously published by Griffiths *et al.* (2018)⁶ and shown here for comparison to related variants.

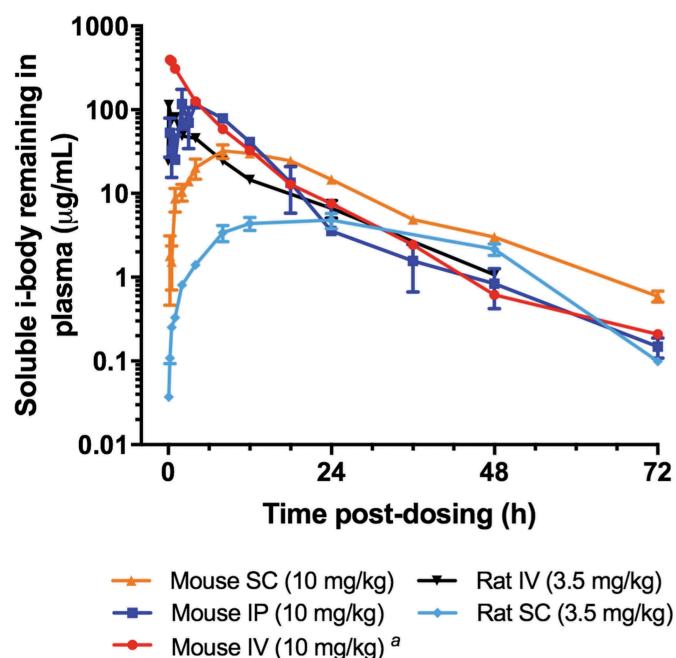


Figure 3. *In vivo* pharmacokinetic data from mice dosed with AD-114-PA600-6H via intraperitoneal (IP), intravenous (IV) or subcutaneous (SC) routes, and rats dosed with AD-114-PA600 (no His₆ tag) via IV or SC routes; showing decrease in the plasma concentration of half-life-extended i-body over time. $N = 3$, error bars show S.E.^a Data previously published by Griffiths *et al.* (2018)⁶ and shown here for comparison to related variants.

0.1, 0.3, then 1 mg/kg, or 3, 10, then 100 mg/kg, all with a 7-day washout period between doses (Table 1, Figure 5b). The fourth study followed a repeat-dose regimen with AD-114-PA600 administered daily for 7 days IV and SC at

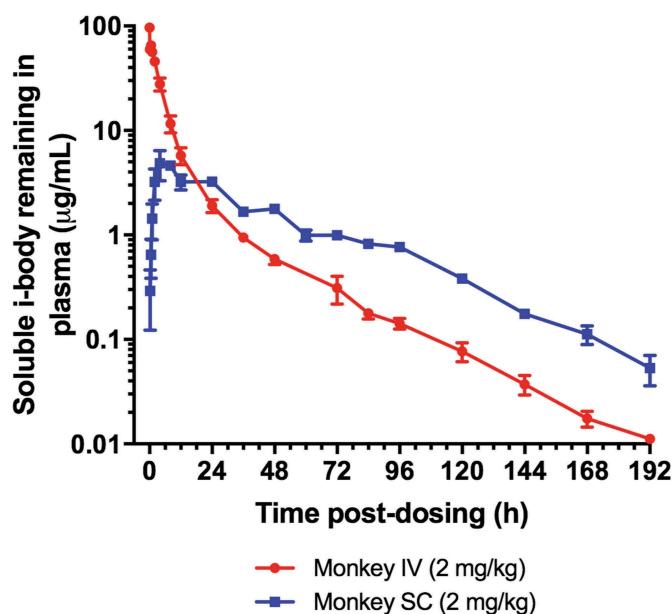


Figure 4. Single dose *in vivo* pharmacokinetic data from cynomolgus monkeys dosed with AD-114-PA600-6H via intravenous (IV, $N = 3$) or subcutaneous (SC, $N = 2$) routes at 2 mg/kg; showing decrease in the plasma concentration of AD-114-PA600-6H over time. Error bars show S.E.

10 mg/kg, and SC at 30 mg/kg (Table 1, Figure 6). We show here that the $t_{1/2}$ of AD-114-PA600 administered IV to cynomolgus monkeys ranged from 6.69 to 24.27 h.

In the NHP studies, as expected, SC administration of AD-114-PA600 resulted in a much lower C_{max} and a longer t_{max} , reflecting the absorption from the injection site (Table 1, Figures 5, 6). In the dose escalation studies, the observed increase in C_{max} and AUC values were roughly proportional to the increase in dose (Table 1, Figure 5). In addition, the observed PK data after repeated administration of AD-114-PA600 (Figure 6) agreed well with the predicted profiles from a PK model fitted to the single dose data (Supplementary S2). Overall, these data suggest that AD-114-PA600 has dose-proportional, linear kinetics, which is time independent. Interestingly, whereas in the single dose NHP study (Figure 4) and in the repeat-dose NHP study (Figure 6) AD-114-PA600 was detected up to 7–14 days after dosing for both IV and SC routes, in the IV NHP dose escalation study (Figure 5a) it was below the lower level of quantification in two of three animals at day 4 and in all animals at day 7. A more rapid loss of exposure at these later time points after treatment with AD-114-PA600 could be explained either by saturation of a clearance process or the formation of anti-drug antibodies, although less likely for IV administration.²² Inclusion of a saturable component to the PK model did not significantly improve the goodness of fit to the observed data, and was unable to explain this observation. The presence of anti-drug antibodies to AD-114-PA600 was not investigated in these studies.

Human allometric scaling

A linear, two-compartment, population PK model was fitted to the observed non-human primate PK data and the model parameters

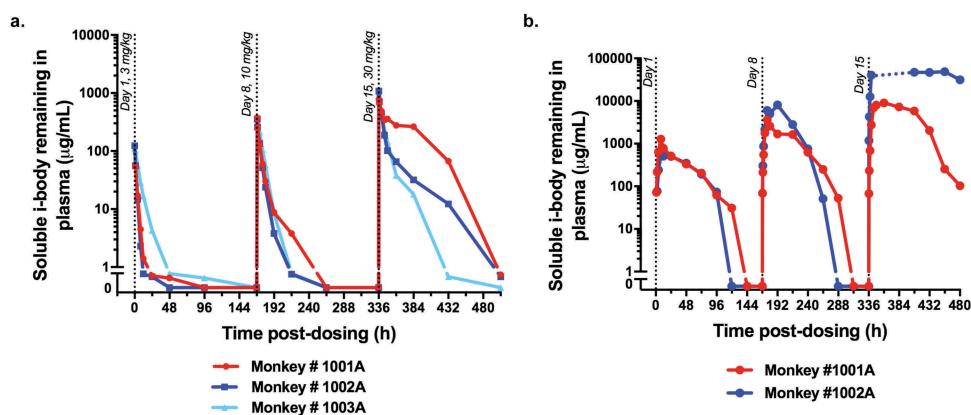


Figure 5. Cynomolgus monkey *in vivo* dose escalation studies.

AD-114-PA600 was administered via the IV route on day 0 at 3 mg/kg, on day 8 at 10 mg/kg and at day 15 at 30 mg/kg (a). AD-114-PA600 was administered via the SC route on days 1, 8, and 15 at 0.1, 1, and 100 mg/kg, respectively (Monkey #1002A, blue line) or at 0.3, 3, or 10 mg/kg, respectively (Monkey #1001A, red line). I-body was above the limit of detection at four timepoints after the day 15 dose in monkey #1002A (dotted line) (b).

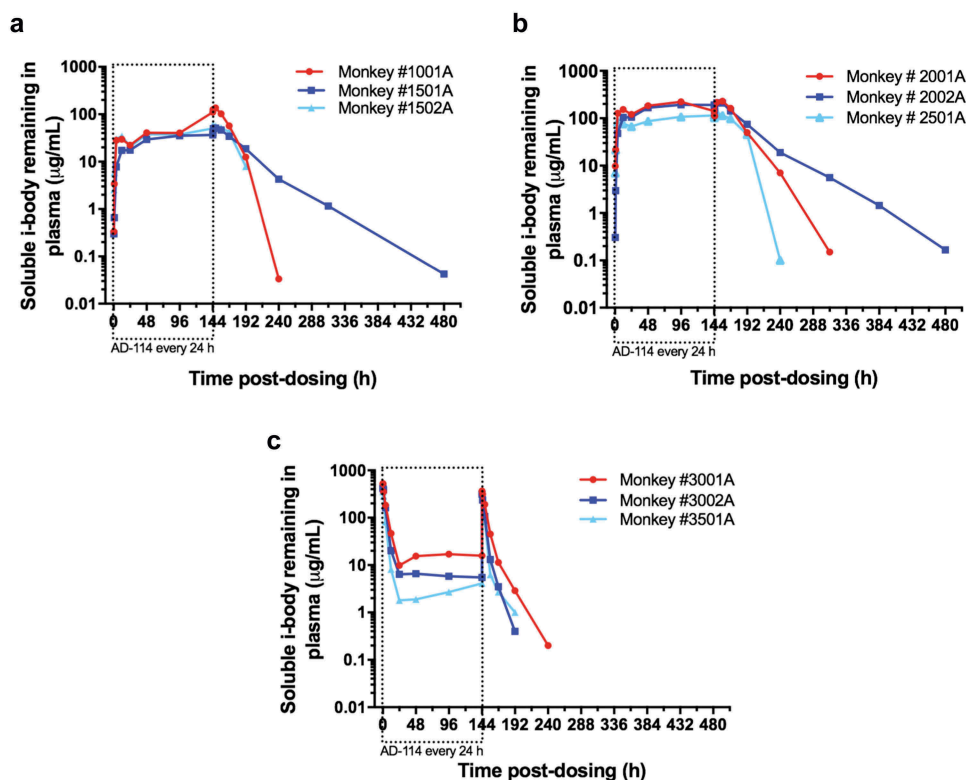


Figure 6. *In vivo* AD-114-PA600 repeat-dose toxicity study in cynomolgus monkeys.

AD-114-PA600 was administered to three animals daily for 7 days via the SC route at 10 mg/kg (a) or at 30 mg/kg (b), or via the IV route for 7 days at 10 mg/kg (c). Dotted vertical lines indicate drug administration times.

were allometrically scaled to humans in order to predict the likely exposure profiles after either SC or IV dosing to human subjects. Based on these simulations, a terminal half-life of 35 h was predicted for AD-114-PA600 in human (Figure 7). The binding affinity of AD-114-PA600 for human CXCR4 suggests that the required concentration for >90% target inhibition/saturation in a static-system (i.e., assuming no target turnover) is at least 1 µg/mL or 0.01 mM, and dosing regimens that would maintain systemic exposure greater than either 1 or 100 µg/mL was simulated (Figure 7). While the human PK modeling depicted in Figure 7a was done for daily SC injection, a terminal half-life of 35 h was

predicted for AD-114-PA600. In fact, this long PK indicates that weekly dosing should be feasible using the PASylated i-body also for SC dosing. For comparison, conventional therapeutic antibodies that require weekly dosing, such as eculizumab (Soliris®) are marketed. Of note, the PASylated i-body would allow convenient self-dosing via SC injection using an autoinjector.

Discussion

The objective of this study was to use several half-life extension technologies to modify the CXCR4-specific i-body AD-114, and

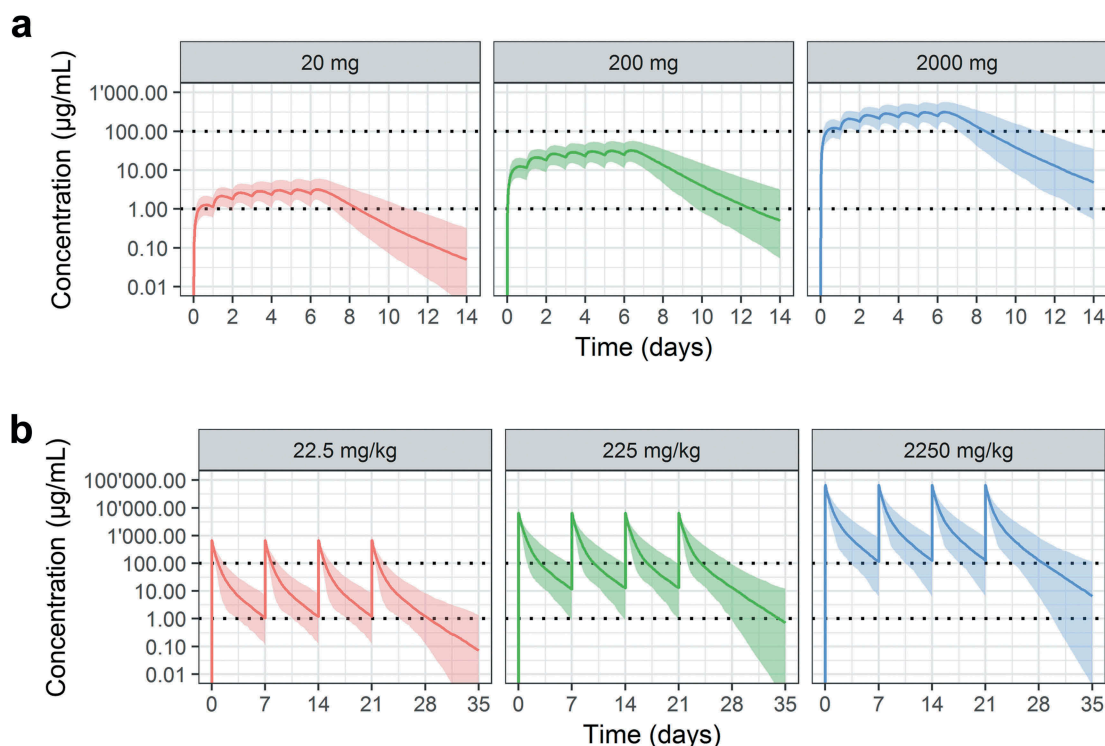


Figure 7. Human modeling.

A two-compartment linear population PK model was fitted to the observed PK NHP data, with drug elimination from the central compartment. This model was then scaled allometrically to simulate the predicted PK profiles in human and for dose rates that would achieve a target serum exposure of 1–100 µg/mL for SC (a) or IV (b) administration routes. Plots are shown for the median, 5th and 95th percentiles of 500 virtual subjects.

to compare PK profiles of the variants in mice, rats, and cynomolgus monkeys. Modification at the C-terminus of AD-114 did not appreciably affect the target affinity for CXCR4 via SPR analysis, consistent with previous observations,⁶ although it did appear to be slightly improved with the addition of PEG. If this is a robust increase, the reason for it is not clear, but this difference in affinity alone is unlikely to be sufficient to affect the half-life of the i-body. Differential binding of the variants to Jurkat cells was observed via flow cytometry, most notably fusion with SA21 and PEG30K correlated with low to negligible cell binding. This may reflect the addition of the C-terminal extension altering either the accessibility of the secondary detection antibody for the His₆ tag, or the i-body's ability to access CXCR4 receptor on the cell surface.

In mice, the greatest improvement in half-life was observed for AD-114-Im7-FH PEG 2 × 20K, followed by AD-114-Im7-FH PEG 30K, AD-114-PA600 and then AD-114-Im7-SA21. It is interesting that we see a rapid clearance followed by a slow clearance after 24 h suggesting that this approach may have potential. Fusion of AD-114 with an HSA-binding i-body domain may have been an interesting comparison, given the half-life of the bispecific Nanobody®, ALX-0061, of 1.44 days in NHP.²³ It should be noted that ALX-0061 would be around double the size of AD-114 and we do not know how the binding affinities to FcRn compare for both these molecules.

A half-life of 7.03 h was observed when AD-114-PA600 was dosed via the IP route, which was shorter than the reported 19.6 h for leptin conjugated to PAS600 (via the N-terminus)²⁴ and may indicate some contribution by receptor-mediated clearance. Although AD-114-Im7-FH PEG 30K had a considerably

longer circulation time than the other variants, losses during manufacturing at the PEG conjugation step meant the variant was difficult to produce in quantities required for dosing larger animals, and any additional chromatography steps to obtain homogenous mono-PEGylated material would have further reduced yields. These findings combined with reports of anti-PEG antibodies and PEG vacuoles^{25,26} in pre-clinical trials for other therapeutic drugs prompted us to pursue PK studies in rats and monkeys using AD-114-PA600, whose production in *E. coli* as protein fusion was sufficiently scalable. In addition, extension of the PA chain length, e.g., to 800 residues, should lead to an even longer half-life.

In NHPs, the half-life of AD-114-PA600 was extended to 24.27 and 25.41 h for IV and SC administration routes, respectively. The increase in mean AUC with increasing dose was overproportional in the ascending dose study (Table 1), although an analysis of PK data across all of the studies indicated that the PK of AD-114-PA600 could be described as both linear and time independent. Including target-mediated disposition, as a saturable component, did not improve the PK model fit to the observed data, although further investigation is required.

The PK data after single doses of AD-114-PA600 were used to predict the PK profiles after repeated administration of AD-114-PA600. Good agreement was observed between predicted and observed data, supporting the conclusion that AD-114-PA600 can be described by a linear PK model. The NHP PK model was allometrically scaled to human and the dosing regimens were designed to achieve a predicted systemic exposure of >1 µg/mL and >100 µg/mL AD-114-

PA600. For a K_d of 3.5 nM (human CXCR4), target occupancy is predicted to be >90% when AD-114-PA600 concentration is >1 $\mu\text{g/mL}$.²⁷ In non-diseased monkeys, the serum concentration of AD-114-PA600 at the target site may be much lower than the systemic concentration owing to the presence of CXCR4 on immune cells, non-specific clearance such as proteolysis, or to target-mediated clearance such as receptor binding, internalization, and proteolysis. Investigating these contributing factors are active areas of research. In particular, it will be important to understand how the PK profiles will be affected if AD-114 is administered to IPF patients given that there have been many reports of CXCR4 being overexpressed in IPF versus non-disease controls.^{17,18}

Whilst *E. coli*-based expression of AD-114-PA600 is cost-effective, additional half-life extension strategies like Fc fusion with expression in mammalian culture should also be considered for the i-body. In the Fc format, avidity effects could improve the apparent affinity of AD-114 for CXCR4, and there would be scope for future development of bispecific molecules. Depot formulations, which enable continuous slow release from polymer or lipid particles, could also be considered.

Material and methods

Protein production

AD-114 fused to Im7-FH, Im7-FH-SA21, PA600 or PA600-His₆ at the C-terminus was expressed in *E. coli* Im7-FH (~12 kDa) is colicin DNase immunity protein⁷²⁸ from *E. coli* fused to Flag and His₆ purification tags, and was used to increase AD-114 expression levels. AD-114-Im7-FH was subsequently C-terminally conjugated to PEG (30K, 2 × 20K, Abzena, UK). The AD-114 sequence was identical in all formats.⁴ AD-114-Im7-FH and AD-114-PA600 ± His₆ were produced as described previously.^{4,6} AD-114-Im7-FH-SA21 was produced as a fusion protein by introducing DNA encoding the HSA-binding peptide SA21²¹ at the N-terminus of AD-114-Im7-FH. The mature protein was expressed in *E. coli* as described previously for AD-114-Im7-FH.⁴

PEGylation of AD-114 was performed via site-specific conjugation of PEG moieties to the C-terminal His₆ purification tag, as described previously by Cong *et al.*¹⁰ AD-114-Im7-FH (1.48 mg/mL, 7.3 mL) in phosphate-buffered saline (PBS, 137 mM sodium chloride, 27 mM potassium chloride, 119 mM phosphate, pH 7.4) was mixed with three mole-equivalent of 30K PEG-bis-sulfone reagent (**Supplementary S3**) in acetonitrile (0.3 mL) and incubated at room temperature overnight with gentle agitation. The reaction mixture was diluted eightfold in 100 mM sodium acetate, pH 4.0 and purified over a HiTrap Macrocap SP column (GE Healthcare #28-9508-59). The column was washed with 10 column volumes of loading buffer to remove residual-unconjugated PEG-bis-sulfone. PEGylated protein was eluted using a 0–100% gradient of elution buffer (100 mM sodium acetate, 1.0 M sodium chloride, pH 4.0). Eluate fractions were analyzed by SDS-PAGE and fractions containing mono- and di-PEGylated species were pooled and concentrated using

a Vivaspin 20 centrifugal device (10K MWCO, Sartorius #VS2002) and then buffer exchanged into PBS to produce a 1:1 mixture of mono-PEGylated and di-PEGylated AD-114-Im7-FH-PEG 30K. Synthesis of 2 × 20K PEGylated AD-114 was prepared via a similar method with the following exceptions: AD-114-Im7-FH in PBS (1.48 mg/mL, 8.1 mL) was added to 2 × 20K PEG-bis-sulfone reagent (**Supplementary S4**), then, following overnight conjugation, purified over a HiLoad Superdex 200 column (GE Healthcare #17-1071-01) using PBS. Mono- and di-PEGylated species were pooled and concentrated, then diluted 12-fold in 100 mM sodium acetate (pH 4.0) and further purified over a HiTrap Macrocap SP column (GE Healthcare #28-9508-59) using a 0–100% elution gradient of 100 mM sodium acetate, 1.0 M sodium chloride, pH 4.0. Eluate fractions containing mono-PEGylated and di-PEGylated species were pooled and concentrated to yield a 1:1 mixture of mono-PEGylated and di-PEGylated AD-114-Im7-FH PEG 2 × 20K.

Surface plasmon resonance

Kinetic binding analysis of all i-bodies was confirmed by SPR as previously described by Griffiths *et al.*⁴ Briefly, using a BIAcore T200 serial dilutions of i-bodies were injected over captured human biotinylated CXCR4 lipoparticles (Integral Molecular # LEV-101B) or human serum albumin (Sigma #A9511). The chip was regenerated between injections for CXCR4 binding experiments with 0.1 M citrate pH 5.0 for 15 sec at 30 $\mu\text{L/min}$. HSA surfaces were regenerated after each binding cycle by a single injection of 10 mM glycine/HCL pH 2.2 at 30 $\mu\text{L/min}$ for 30 sec.

Flow cytometry

Jurkat cells were cultured in RPMI-1640 (Gibco # 11875093) + 10% v/v FBS (Bovagen #SFBS-NZ) at 37°C and 5% CO₂. Cells were labelled with each i-body variant at a final concentration of 1 μM for 10 min at room temperature, washed with PBS (150 μL) and then stained with secondary antibody anti-His-APC (R&D Systems #IC050A) for 10 min at room temperature. Cells were washed again with PBS (150 μL) and resuspended in PBS. A CytoflexS (Beckman Coulter) flow cytometer was utilized for analysis, and data were analyzed using FlowJo software version 7.6 (Treestar Inc.).

Pharmacokinetic studies

In vivo PK studies were conducted at ITR Laboratories Canada Inc. in accordance with the principles outlined in the “Guide to the Care and Use of Experimental Animals” as published by the Canadian Council on Animal Care and the NIH’s “Guide for the Care and Use of Laboratory Animals”. The studies were approved by the Animal Care Committee (ACC) of ITR Laboratories Canada Inc., and ACC acceptance of the study plans was maintained on file at ITR Laboratories Canada Inc. Mice [Male Crl:CD1 (ICR) (Charles River Canada Inc.)], rats [Sprague-Dawley Crl:CD (SD) (Charles River Canada Inc.)] and cynomolgus monkeys

(*Macaca fascicularis*, Worldwide Primates Inc.) were housed individually in a controlled environment of $21 \pm 3^\circ\text{C}$, relative humidity $50 \pm 20\%$, 12 h light, 12 h dark. Blood samples were taken via the saphenous vein or under isoflurane anesthesia by cardiac puncture (0.1–0.3 mL, mice), jugular venipuncture (0.3 mL, rats) or femoral or brachial venipuncture (0.6 mL, monkeys), using $\text{K}_2\text{-EDTA}$ as anti-coagulant. Blood samples were centrifuged at 4°C and the resulting plasma was stored at -80°C in Protein LoBind tubes (Eppendorf #0030108116). At the end of the study, mice, and rats were euthanized by cervical dislocation and discarded without further examination, whilst monkeys were released into the spare colony at ITR Laboratories Canada Inc.

Study 1 (Figure 2)

AD-114-Im7-FH-SA21, AD-114-PEG-2 \times 20K and -PEG30K pharmacokinetic studies in mice

Mice were injected IV with a single dose of i-body. AD-114-Im7-FH, AD-114-Im7-FH-SA21, and AD-114-PEG 30K were dosed at 3, 2 and 3 mg/kg, respectively, and blood samples were collected 5 min, 2, 6, 12, 24, 72 h post dosing. AD-114-PEG 2 \times 20K was dosed at 1.25 mg/kg and blood samples were collected 5 min, 2, 6, 12, 24, 72, 120, 144 h post dosing. Dose rates were at the highest possible concentration, given the availability of each variant type. AD-114 variants were quantified by monitoring the signature framework peptide LTPNQQR in plasma using liquid chromatography-mass spectrometry (LC-MS)/MS (XBridge BEH300 C18, 50×2.1 mm, $3.5 \mu\text{m}$ reverse phase chromatography column and AB Sciex QTRAP5500 triple quadrupole mass spectrometer), as described previously.⁶

Study 2 (Figure 3) AD-114-PA600-6H pharmacokinetic studies in mice and rats

AD-114-PA600-6H at 10 mg/kg was administered to mice SC or IP, and blood samples were collected at 15, 30 min, 1, 2, 3, 4, 8, 12, 18, 24, 36, 48 and 72 h post dosing. Plasma samples were diluted 1/10 in 1% (w/v) BSA (Sigma #A7030) in PBS and AD-114-PA600-6H was quantified by enzyme-linked immunosorbent assay (ELISA) as described previously using anti-human NCAM-1 (R&D Systems #MAB2408) to capture i-body and anti-Histidine-HRP (BioRad #MCA1396P) to detect His₆ tagged i-body. Rats were injected IV or SC with AD-114-PA600-6H at 3.5 mg/kg. Following IV dosing, blood samples were collected immediately post dosing and at 5, 30 min, 2, 8, 24, 72 h post dosing. Following SC dosing, blood samples were collected at 5, 15, 30 min, 1, 2, 4, 8, 12, 24, 48, 72, 96 h post dosing. AD-114-PA600-6H was quantified in plasma by LC-MS/MS as outlined above and described previously.⁶

Study 3 (Figure 4) AD-114-PA600-6H pharmacokinetic study in cynomolgus monkeys (*Macaca fascicularis*)

AD-114-PA600-6H at 2 mg/kg was administered to monkeys IV and SC, and blood samples were collected immediately following dosing and at 5, 15, and 30 min and 1, 2, 4, 8, 12, 24,

36, 48, 60, 72, 84, 96, 120, 144, 168, and 192-h post-dosing. AD-114-PA600-6H was quantified in plasma by LC-MS/MS as outlined above and described previously.⁶

Study 4 (Figure 5) AD-114-PA600 dose escalation toxicity studies in cynomolgus monkeys

AD-114PA600 was administered to cynomolgus monkeys in two dose escalation regimens, with a 7-day observation period between dosing occasions. In the first regimen, each of three animals was dosed IV on day 1 at 3 mg/kg, on day 8 at 10 mg/kg, and on day 15 at 30 mg/kg. Blood samples were collected pre-dosing and at the following time points post-dosing: 5 min, 1, 4, 12, 24, 48, 96, 168 h. In the second regimen, AD-114PA600 was administered SC to one animal on days 1, 8 and 15 at 0.1, 1, 100 mg/kg, respectively, or to a separate single animal at 0.3, 3 and 10 mg/kg, respectively. Blood samples were collected pre-dosing and at the following time points post each dosing: 30 min, 1, 2, 4, 8, 12, 24, 48, 72, 96, 120, and 144 h. For both studies, AD-114-PA600 was quantified in plasma by LC-MS/MS as outlined above and described previously.⁶

Study 5 (Figure 6) AD-114-PA600 repeat-dose toxicity study in cynomolgus monkeys

AD-114-PA600 was administered daily to monkeys ($N = 3$ per group) by SC or IV injection for 7 consecutive days. Dose rates were 10 mg/kg for the IV route, 10 and 30 mg/kg for the SC route. Blood samples were collected on Day 1 and 7 at the following time points: pre-dose, 5 (IV route only) or 30 min (SC route only) and 1, 4, 12, 24, 48, 96, and 144-h post-dose; in addition, blood was collected at 168, 240 and 336-h post-dose on Day 7 only. AD-114-PA600 was quantified in plasma by LC-MS/MS as outlined above and described previously.⁶

Pharmacokinetic analysis

Non-compartmental analysis of the AD-114 plasma concentration data sets was conducted using the Phoenix WinNonlin (CertaraTM, Version 6.3) software using the following configuration for analysis: Sampling Method, Sparse for mouse and rat studies, Rich for NHP studies; AUC Calculation Method, Linear Trapezoidal with Linear Interpolation, Lambda Z (λ_z) Method, Best fit for λ_z , Log regression; Weighting (λ_z calculation), Uniform. PK parameters (including abbreviation and description for each parameter) are as follows: $t_{1/2}$ (terminal elimination half-life); C_{max} (the maximum plasma concentration), t_{max} (time to maximum plasma concentration).

Compartmental PK analysis and allometric scaling to human and simulations

The PK data were analyzed using a non-compartmental approach (see above). In addition, a two-compartment linear population PK model was fitted to the observed PK NHP data, with drug elimination from the central compartment (**Supplementary S5**). This model described the observed data sufficiently well (**Supplementary S6**), and the goodness

of fit was not significantly improved by adding a saturable clearance process. The observed volume of distribution and clearance were scaled with exponents of 1.0 and 0.8, respectively, and the inter-compartmental exchange coefficient was scaled with an exponent of 0.67. The rate of absorption and systemic bio-availability from SC administration were assumed to be similar for NHP and human. 500 PK profiles in human were simulated with patient variability and summarized with the median, 5th and 95th percentiles. Population PK parameters were estimated with Monolix (Monolix version 2016R1. Antony, France: Lixoft SAS, 2016. <http://monolix2016.lixoft.com>) and simulations were run in R (R Development Core Team (2008). R: A language and environment for statistical computing. R Foundation for Statistical Computing, Vienna, Austria. ISBN 3-900051-07-0, URL <http://www.Rproject.org>) using the mlxR library (Marc Lavielle, 2017, mlxR: Simulation of Longitudinal Data. R package. <http://simulx.webpopix.org>).

Statistical analysis

All data were analyzed using GraphPad Prism (version 7).

Data availability

The datasets generated during the current study are available from the corresponding author on reasonable request.

Abbreviations

ACC	Animal Care Committee
AUC	area under the curve
BSA	bovine serum albumin _{C_{max}} , maximum concentration
CXCR4	C-X-C chemokine receptor 4
FBS	fetal bovine serum
FcRn	neonatal Fc receptor
HRP	horseradish peroxidase
HSA	human serum albumin
Im7	colicin immunity protein 7
IP	intraperitoneal
IV	intravenous
LC-MS/MS	liquid chromatography-mass spectrometry
mAb	monoclonal antibody
NHP	non-human primate
PA	proline/alanine repeat motif for half-life extension
PAS	proline/alanine-rich sequence for half-life extension
PBS	phosphate-buffered saline
PEG	polyethylene glycol
PK	pharmacokinetic
SC	subcutaneous
SE	standard error
SPR	surface plasmon resonance
t _{1/2}	half-life
t _{max}	time to reach maximum concentration
V _{NAR}	shark variable new antigen receptor
XTEN [®]	XTEN [®] half-life extension

Acknowledgments

We thank the LIMS BioImaging Facility at La Trobe University for access to flow cytometers. We thank Dr Olan Dolezal (Manufacturing Flagship, Commonwealth Scientific and Industrial Research Organization) and Dr Menachem Gunzburg (Monash FBDD Platform, Monash University) for SPR analyses. We thank Ebony Fietz, Angus Tester,

Dallas Hartman and Samantha Cobb for valuable discussions and proofreading.

Author contributions

M.Foley, K.G., U.B., A.S., M.Frigerio, R.T and W.M. designed the research. K.G., U.B., W.D., M.Frigerio, R.T and W.M. performed the research. K.G., M.Foley, P.L., M.M., L.R., A.S., U.B., M.Frigerio, R.T, W. M. and W.D. analyzed the data. K.G., M.Foley, P.L., M. Frigerio, C. H. and W.D. wrote the paper. All authors reviewed the results and approved the final version of the manuscript.

Competing Financial Interests Statement

M. Foley is a shareholder of AdAlta Ltd. W.D. and C.H. salaries are funded by AdAlta Ltd. U.B. and A.S. are shareholders of XL-protein GmbH. M. Frigerio and W.M. salaries are funded by Abzena. R.T. salary is funded by Lonza Biologics. P.L., M.M. and L. R. are independent consultants and were funded by AdAlta Ltd. Some authors have non-financial relationships with entities in the biomedical arena that could be perceived to influence, or that give the appearance of potentially influencing, what is written in this work. K.G. and M. Foley have issued patents relating to the reported work.

ORCID

Katherine Griffiths  <http://orcid.org/0000-0003-0580-1125>
 William McDowell  <http://orcid.org/0000-0002-4893-9784>
 Mark Frigerio  <http://orcid.org/0000-0002-5954-0488>
 William G. Darby  <http://orcid.org/0000-0001-6051-4175>
 Arne Skerra  <http://orcid.org/0000-0002-5717-498X>

References

- Kaplon H, Reichert JA-O. Antibodies to watch in 2019. *Mabs*. 2019 Feb/Mar;11(2):219–38. doi:10.1080/19420862.2018.1556465.
- Bannas P, Hambach J, Koch-Nolte F. Nanobodies and nanobody-based human heavy chain antibodies as antitumor therapeutics. *Front Immunol*. 2017;8:1603. doi:10.3389/fimmu.2017.01603.
- Kovaleva M, Ferguson L, Steven J, Porter A, Barelle C. Shark variable new antigen receptor biologics - a novel technology platform for therapeutic drug development. *Expert Opin Biol Ther*. 2014;14:1527–39. doi:10.1517/14712598.2014.937701.
- Griffiths K, Dolezal O, Cao B, Nilsson SK, See HB, Pflieger KD, Roche M, Gorry PR, Pow A, Viduka K, et al. i-bodies, human single domain antibodies that antagonize chemokine receptor CXCR4. *J Biol Chem*. 2016;291:12641–57. doi:10.1074/jbc.M116.721050.
- Mujic-Delic A, de Wit RH, Verkaar F, Smit MJ. GPCR-targeting nanobodies: attractive research tools, diagnostics, and therapeutics. *Trends Pharmacol Sci*. 2014;35:247–55. doi:10.1016/j.tips.2014.03.003.
- Griffiths K, Habel DM, Jaffar J, Binder U, Darby WG, Hosking CG, Skerra A, Westall GP, Hogaboam CM, Foley M. Anti-fibrotic effects of CXCR4-Targeting i-body AD-114 in pre-clinical models of pulmonary Fibrosis. *Sci Rep*. 2018;8:3212. doi:10.1038/s41598-018-20811-5.
- Kontermann RE. Half-life extended biotherapeutics. *Expert Opin Biol Ther*. 2016;16:903–15. doi:10.1517/14712598.2016.1165661.
- Kontermann RE. Strategies for extended serum half-life of protein therapeutics. *Curr Opin Biotechnol*. 2011;22:868–76. doi:10.1016/j.copbio.2011.06.012.
- Veronese FM, Mero A. The impact of PEGylation on biological therapies. *Biodrugs*. 2008;22:315–29. doi:10.2165/00063030-200822050-00004.
- Cong Y, Pawlisz E, Bryant P, Balan S, Laurine E, Tommasi R, Singh R, Dubey S, Peciak K, Bird M, et al. Site-specific PEGylation

- at histidine tags. *Bioconjug Chem.* 2012;23:248–63. doi:10.1021/bc200530x.
11. Binder U, Skerra A. PASylation[®]: A versatile technology to extend drug delivery. *Curr Opin Colloid In.* 2017;31:10–17. doi:10.1016/j.cocis.2017.06.004.
 12. Podust VN, Balan S, Sim BC, Coyle MP, Ernst U, Peters RT, Schellenberger V. Extension of in vivo half-life of biologically active molecules by XTEN protein polymers. *J Control Release.* 2016;240:52–66. doi:10.1016/j.jconrel.2015.10.038.
 13. Li H, d'Anjou M. Pharmacological significance of glycosylation in therapeutic proteins. *Curr Opin Biotechnol.* 2009;20:678–84. doi:10.1016/j.copbio.2009.10.009.
 14. Huang C. Receptor-Fc fusion therapeutics, traps, and MIMETIBODY technology. *Curr Opin Biotechnol.* 2009;20:692–99. doi:10.1016/j.copbio.2009.10.010.
 15. Hutt M, Farber-Schwarz A, Unverdorben F, Richter F, Kontermann RE. Plasma half-life extension of small recombinant antibodies by fusion to immunoglobulin-binding domains. *J Biol Chem.* 2012;287:4462–69. doi:10.1074/jbc.M111.311522.
 16. Sleep D, Cameron J, Evans LR. Albumin as a versatile platform for drug half-life extension. *Biochim Biophys Acta.* 2013;1830:526–34. doi:10.1016/j.bbagen.2013.04.023.
 17. Strieter RM, Gomperts BN, Keane MP. The role of CXC chemokines in pulmonary fibrosis. *J Clin Invest.* 2007;117:549–56. doi:10.1172/JCI30562.
 18. Xu J, Mora A, Shim H, Stecenko A, Brigham KL, Rojas M. Role of the SDF-1/CXCR4 axis in the pathogenesis of lung injury and fibrosis. *Am J Respir Cell Mol Biol.* 2007;37:291–99. doi:10.1165/rcmb.2006-0187OC.
 19. Feng Y, Broder CC, Kennedy PE, Berger EA. HIV-1 entry cofactor: functional cDNA cloning of a seven-transmembrane, G protein-coupled receptor. *Science.* 1996;272:872–77.
 20. Moll NM, Ransohoff RM. CXCL12 and CXCR4 in bone marrow physiology. *Expert Rev Hematol.* 2010;3:315–22. doi:10.1586/ehm.10.16.
 21. Dennis MS, Zhang M, Meng YG, Kadkhodayan M, Kirchofer D, Combs D, Damico LA. Albumin binding as a general strategy for improving the pharmacokinetics of proteins. *J Biol Chem.* 2002;277:35035–43. doi:10.1074/jbc.M.205854200.
 22. Hamuro L, Kijanka G, Kinderman F, Kropshofer H, Bu DX, Zepeda M, Jawa V. Perspectives on subcutaneous route of administration as an immunogenicity risk factor for therapeutic proteins. *J Pharm Sci.* 2017;106:2946–54. doi:10.1016/j.xphs.2017.05.030.
 23. Van Roy M, Ververken C, Beirnaert E, Hoefman S, Kolkman J, Vierboom M, Breedveld E, 'T Hart B, Poelmans S, Bontinck L, et al. The preclinical pharmacology of the high affinity anti-IL-6R Nanobody(R) ALX-0061 supports its clinical development in rheumatoid arthritis. *Arthritis Res Ther.* 2015;17:135. doi:10.1186/s13075-015-0651-0.
 24. Morath V, Bolze F, Schlapschy M, Schneider S, Sedlmayer F, Seyfarth K, Klingenspor M, Skerra A. PASylation of murine leptin leads to extended plasma half-life and enhanced in vivo efficacy. *Mol Pharm.* 2015;12:1431–42. doi:10.1021/mp5007147.
 25. Ivens IA, Achanzar W, Baumann A, Braendli-Baiocco A, Cavagnaro J, Dempster M, Depelchin BO, Rovira ARI, Dill-Morton L, Lane JH, et al. PEGylated biopharmaceuticals: current experience and considerations for nonclinical development. *Toxicol Pathol.* 2015;43:959–83. doi:10.1177/0192623315591171.
 26. Turecek PL, Bossard MJ, Schoetens F, Ivens IA. PEGylation of biopharmaceuticals: a review of chemistry and nonclinical safety information of approved drugs. *J Pharm Sci.* 2016;105:460–75. doi:10.1016/j.xphs.2015.11.015.
 27. Lowe PJ, Tannenbaum S, Wu K, Lloyd P, Sims J. On setting the first dose in man: quantitating biotherapeutic drug-target binding through pharmacokinetic and pharmacodynamic models. *Basic Clin Pharmacol Toxicol.* 2010;106:195–209. doi:10.1111/j.1742-7843.2009.00513.x.
 28. Hosse RJ, Tay L, Hattarki MK, Pontes-Braz L, Pearce LA, Nuttall SD, Dolezal O. Kinetic screening of antibody-Im7 conjugates by capture on a colicin E7 DNase domain using optical biosensors. *Anal Biochem.* 2009;385:346–57. doi:10.1016/j.ab.2008.11.026.